Oceanologia (2017) 59, 166—176

Available online at www.sciencedirect.com

ScienceDirect

journal homepage: www.journals.elsevier.com/oceanologia/

ORIGINAL RESEARCH ARTICLE

Toward downscaling oceanic hydrodynamics — suitability of a high-resolution OGCM for describing regional ocean variability in the South China Sea

Meng Zhang*, **Hans von Storch**

Institute for Coastal Research, Helmholtz Zentrum Geesthacht, Geesthacht, Germany

Received 22 June 2016; accepted 4 January 2017
Available online 18 January 2017

KEYWORDS
Ocean downscaling;
STORM;
The South China Sea

Summary We suggest to transfer the empirical downscaling methodology, which was developed mostly for atmospheric dynamics and impacts, to regional ocean problems. The major problem for doing so is the availability of decades-long and homogeneous and spatially detailed data sets. We have examined the performance of the STORM multidecadal simulation, which was run on a 0.1° grid and forced with 1950—2010 NCEP re-analyses, in the South China Sea and found the data suitable. For demonstration we build with this STORM-data downscaling model for the regional throughflow.

The STORM data is compared with AVISO satellite observations and the ocean re-analysis dataset C-GLORS. We find the seasonal patterns and the inter-annual variability of sea surface height anomaly in both the C-GLORS data and the STORM simulation consistent with the AVISO-satellite data. Also the strong westward intensification and the seasonal patterns of South China Sea circulation steered by the monsoon have been presented well. As an important indicator of vertical movement, the sea surface temperature distribution maps are also very close, especially for the narrow upwelling region in summer. We conclude that the output of the STORM simulation is realistically capturing both the large-scale as well as the small-scale dynamical features in the South China Sea.

* Corresponding author at: Helmholtz-Zentrum Geesthacht Centre for Materials and Coastal Research, Max-Planck-Str. 1, 21502 Geesthacht, Germany. Tel.: +49(0)4152 87-1851; fax: +49(0)4152 87-2832.
E-mail address: meng.zhang@hzg.de (M. Zhang).

Peer review under the responsibility of Institute of Oceanology of the Polish Academy of Sciences.

ELSEVIER | Production and hosting by Elsevier

http://dx.doi.org/10.1016/j.oceano.2017.01.001

1. Introduction

As the largest semi-enclosed marginal sea located in the southeast Asian waters, the South China Sea (SCS) covers an area of about 3.5 million km^2 in total, with an average depth more than 2000 m and a maximum depth of about 5000 m. It is surrounded by China, Vietnam, Philippine Islands, Malaysia and other countries. Via the Luzon Strait, Taiwan Strait and the Strait of Malacca, it connects the Pacific Ocean, East China Sea and Indian Ocean (Fang et al., 2006a, b, 2012; Ho et al., 2000; Hu et al., 2000; Li et al., 2003).

Due to the influence of the East Asian monsoon system, the SCS circulation represents significant seasonal characteristics. Previous studies have been carried out to analyze the features of the SCS circulation. Dale (1956) determined the SCS surface circulation in winter and summer for the first time from the ship drift data, which clearly revealed the seasonal differences. Wyrtki (1961) pointed out that the monsoon is the main driver of the SCS circulation.

The advent of satellite remote sensing technology allowed the analysis of the details of the SCS circulation. Ho et al. (2000) has described the seasonal variability of sea surface height (SSH) based on the TOPEX/Poseidon altimeter data during 1992–1997. Fang et al. (2006b) used the gridded 11-year AVISO SSH data, which merged data from TOPEX/Poseidon, ERS and Jason, for characterizing the low frequency variability of the SCS surface circulation and to discuss its relationship with El Niño-Southern Oscillation. The conclusion of the annual variability responding to the change of monsoon was confirmed by their study.

Recently, several numerical simulations of the SCS circulation were done. Such simulations help extend our knowledge about past variations beyond the short time period of satellite observations and beyond the sparse sampling of in situ observation and ship observation. Wei et al. (2003) embedded a fine-grid ocean model of the China Sea into a global model so that open boundary conditions were no longer needed. Their modeled monthly SSH anomalies (SSHA) were similar to the TOPEX/Poseidon data, and the model could seasonably reproduce the SCS Southern Anticyclonic Gyre in summer and the SCS Southern Cyclonic Gyre in winter. Using this model, the seasonal features of the water intruding into the SCS through the Luzon Strait in different ocean layers were investigated. Wang et al. (2006) modeled the interannual variability of the SCS circulation and its relation to wind stress and El Niño through on an irregular grid. Such numerical simulations allowed the detailed study of processes and physical mechanisms of some mesoscale phenomena, for example, the topographical effect on the coastal upwelling in the north SCS (Wang et al., 2012, 2014).

In spite of those signs of progress, a systematic, detailed, homogeneous and comprehensive description of the SCS circulation on regional and local scales across several decades is hardly available. The "empirical downscaling" methodology may help to generate such descriptions, which will also allow for detection externally driven change as well as projecting possible future change on such regional scales. Most downscaling efforts were directed at atmospheric phenomena (Benestad et al., 2008; von Storch et al., 1993), but a few oceanic applications dealing with local sea level were presented in the 1990s (Cui et al., 1995; von Storch and Reichardt, 1997).

An alternative to empirical downscaling is dynamical downscaling using regional dynamical models (oceanographic examples are provided by Kauker and von Storch, 2000; Schrum et al., 2003); however, this approach is more challenging and cost-intensive than the empirical approach; also the empirical approach may deal with local phenomena, which are possibly less well resolved by dynamical models. Therefore, we explore the potential of the empirical downscaling of oceanic dynamics.

For doing so for the South China Sea (SCS), we need a consistent and homogeneous description of the regional space-time variability in that region. As a first preparational step, we examine the suitability of a multidecadal global simulation "STORM" with the MPI-OM, the high-resolution global ocean model of the Max Planck Institute of Meteorology (MPI; Li and von Storch, 2013; von Storch et al., 2012), which was forced by NCEP atmospheric re-analyses.

The high resolution of about 1/10° makes STORM capable to describe the small-scale features, while the temporal coverage over 60 years enables STORM to analyze the long-term variability of the SCS circulation. In addition, STORM provides the large-scale states. Therefore, STORM is a good choice for constructing the statistical relationship between large and small scales. Also all relevant second-moment statistics have been archived by accumulating two-variable-products at every time step (von Storch et al., 2012).

In this paper, we first assess the performance of STORM in describing the SCS circulation, by comparing with AVISO altimeter measurements and ocean re-analysis dataset C-GLORS. In Section 2, these three data sets are described in detail. Section 3 presents the comparisons, in terms of sea surface height anomalies (SSHA), surface current and sea surface temperature (SST). Eventually, for demonstration, an empirical downscaling model has been constructed (Section 4), which allows deriving the monthly seasonal near-surface regional throughflow in the South China Sea from the regional wind fields.

2. Dataset description

2.1. Satellite observations

The monthly SSALTO (SSALTO multimission ground segment)/Duacs (Data Unification and Altimeter Combination System) gridded SSHA (sea surface height anomaly) data set from Archiving, Validation and Interpretation of Satellite Data in Oceanography (AVISO) covers almost the entire global ocean with a resolution of 0.25° from 1993 to 2014. It has been built from several satellite products, including TOPEX-POSEIDON, ERS, JASON and ENVISAT (AVISO, 1996, 2009).

As a consequence of its high quality, the AVISO SSHA data has often been used as reference to validate global model output and characterize regional currents (Fang et al., 2006a,b). In this paper, we compare the AVISO SSHA data with SSHA from the STORM simulation and the ocean re-analysis C-GLORS.

2.2. The ocean re-analysis dataset C-GLORS

The ocean reanalysis dataset C-GLORS (version 4) has the same horizontal 0.25° grid resolution as AVISO. It has been

produced by the global ocean re-analysis system of CMCC (The Euro-Mediterranean Center for Climate Change), which has assimilated in situ observations of temperature, salinity (from moorings and ARGO floats) and sea surface height (from AVISO satellite data; Storto and Masina, 2014; Storto et al., 2016).

The monthly dataset from 1982 to 2013 can be downloaded from their website http://www.cmcc.it/c-glors/.

2.3. The STORM/NCEP simulation

Three high-resolution global ocean-only simulation STORM from the German STORM consortium employed the state-of-the-art model MPI-OM and was forced by the NCEP-NCAR reanalysis data (Li and von Storch, 2013; Tim et al., 2015; von Storch et al., 2012). This simulation operates with a tri-polar grid — with a very fine grid spacing of about 0.1° and only 2.3 km at the finest grid, and 80 unevenly distributed levels in vertical. The simulation was run for 6 decades of years, 1950—2010. For fair comparison, STORM was interpolated on a horizontal 0.25°-grid.

Several aspects of the STORM simulation data have been examined, such as the oceanic Lorenz energy cycle for the World Ocean (von Storch et al., 2012), the sea surface temperature (SST) near Benguela current as well as the decadal variability and trends of the upwelling system there (Tim et al., 2015). The simulation was found to be mostly realistic, even if some biases prevailed.

3. Assessing the realism of the STORM data

The three data sets, STORM, C-GLORS and AVISO cover different variables, and descriptions for different time windows. The satellite AVISO contains only sea surface height for 1993—2014, while the re-analysis C-GLORS provide the full range of dynamical variables for 1982—2013 and STORM for 1950—2010.

We consider AVISO as the data set closest to reality; thus we examine first, how well the derived products C-GLORS and STORM compare with AVISO. The realism of C-GLORS in terms of SSHA, leads us to assessing the quality of STORM with respect to other variables by comparing it with C-GLORS. The first step demonstrates the suitability of using all C-GLORS variables; the second step suggests that STORM provides a realistic description across the 60 year time window 1950—2012.

3.1. SSHA in AVISO, C-GLORS and STORM

SSHA is often used to analyze the ocean dynamics and the upper layer circulation (Cheng et al., 2016; Fang et al., 2006b; Li et al., 2003; Wei et al., 2003). This data is available from AVISO in 1993—2014. For the comparisons with C-GLORS and STORM, the joint period from 1993 to 2010 has been chosen.

The observed AVISO-SSHA is the actual state subject to the influences of dynamical, eustatic and steric effects, whereas the modeled SSHA from STORM and C-GLORS only describe the dynamical effects and not eustatic and steric effects. According to the fifth report of IPCC (IPCC, 2013), the growth of the global mean sea level since the 1970s is mostly caused by the thermal expansion of global warming and glacier loss. For removing the difference influenced by eustatic and steric effect, we subtract the trend of AVISO. In case that the trend related to dynamical effect is removed as well, for fair comparison, SSHA from C-GLORS and STORM are also detrended.

The climatological seasonal mean states of detrended SSHAs of STORM and C-GLORS (Fig. 1) show good agreement with AVISO. In winter (DJF), basin-wide low SSHAs control the east part of the SCS, which presents the cyclonic currents in the upper layer in the whole SCS. Furthermore, in these three datasets, two low SSHA centers located in the north and south SCS respectively. In summer (JJA), the situation is just opposite. Anti-cyclonic currents dominate the SCS region in all the three datasets, however a maximum SSHA over 0.1 m appears near the Luzon Strait in AVISO and C-GLORS, which is a little lower in STORM.

The (temporal) standard deviation of the seasonal means represents interannual variability. The patterns of detrended SSHA standard deviation distributions (Fig. 2) for the four seasons of three datasets are similar. As December in 1992 is not available, there are only 17 months in winter (DJF), but 18 months in other three seasons. All of them show that, in winter and spring, the deviation near Luzon Strait is always higher than adjacent seas, and in summer and autumn, strong variability centers in the Vietnam's coast water. Compared with AVISO and C-GLORS, the STORM simulates stronger variability in Luzon Strait in summer and autumn, yet weaker variability in the Vietnam coast in spring. In summer, the area of the center with strong variability near Vietnam is closer to AVISO, compared with C-GLORS.

Empirical Orthogonal Functions (EOF) decompose the time series of SSHA fields, several orthogonal modes capture the main variability (von Storch and Zwiers, 1999; Wang et al., 2006). We apply the EOF decomposition to the three detrended datasets, after removing the mean annual cycle (by subtracting a multi-year monthly average). The EOFs have been normalized so that the standard deviation of the time coefficients (principal component, PC) is 1 — so that the different intensity of the EOFs is given by the patterns.

The main feature of the first EOF pattern (EOF1; Fig. 3) describes an overall simultaneous in- or decrease in the SCS. The amplitude in the east is greater than it in other regions. The EOF1s of C-GLORS and STORM are generally consistent with AVISO. However, a small negative center with small area and weak intensity appears in C-GLORS and three similar centers occur in STORM. Seen from the figures, also the EOF time series for three datasets vary similarly. The time series in C-GLORS and STORM closely correlate with AVISO, with the correlation coefficients of 0.94 and 0.91, respectively. In 1997, SSHAs in all three datasets dropped suddenly and then rebounded quickly in 1998. With respect to the represented percentage of the variance, 25.1% in STORM is closer to 27.0% in AVISO, than 36.6% in C-GLORS.

The second EOF (EOF2) patterns in three datasets all show a strong anti-cyclonic gyre located off the Vietnam coast and extending northeastward to reach Philippine Islands, covering most part of the north SCS. The remaining areas are associated with negative value. The coverage of intensity over 0.05 m in STORM is larger than that in AVISO, while the positive values in C-GLORS are all under 0.05 m. The

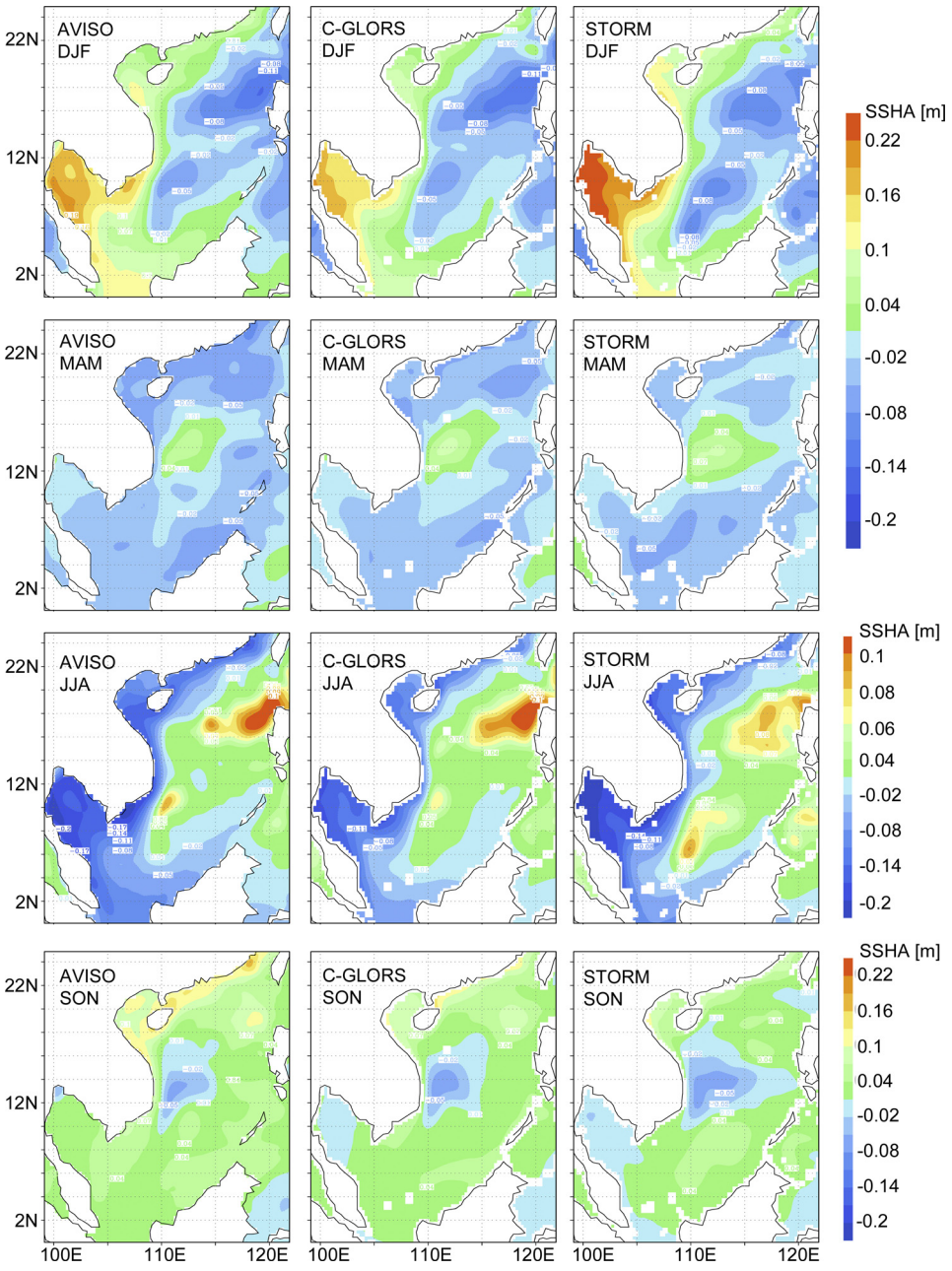

Figure 1 1993—2010 seasonal means of detrended sea surface height anomalies (SSHA) [m] according to AVISO, C-GLORS and STORM. From top to bottom: DJF, MAM, JJA and SON.

percentages of variance described by both STORM and C-GLORS are greater than AVISO. Their EOF2 coefficient time series of C-GLORS and STORM show correlations with AVISO 0.80 and 0.77, respectively.

Our analysis demonstrates that C-GLORS and STORM have the ability to capture the main variability features of the SCS dynamics in terms of seasonal variance and interannual variability of SSHA. C-GLORS shows greater similarity, which is not surprising as it has assimilated AVISO satellite data. We think the similarity of SSHA in AVISO and C-GLORS points to the plausibility that also other parameters of C-GLORS may be considered mostly realistic. Therefore, we will continue assessing STORM, with C-GLORS as a reference, in the following chapter. In the following, we assess the description of surface currents and SST in the joint period 1982—2010 shared by C-GLORS and STORM.

3.2. Surface current fields in C-GLORS and STORM

The first level for ocean horizontal current fields in STORM is at 6 m depth, so we choose this level as surface to perform comparison and get the C-GLORS currents at 6 m depth through vertical interpolation.

The seasonal mean surface current fields of STORM and C-GLORS (Fig. 4) show similar variability.

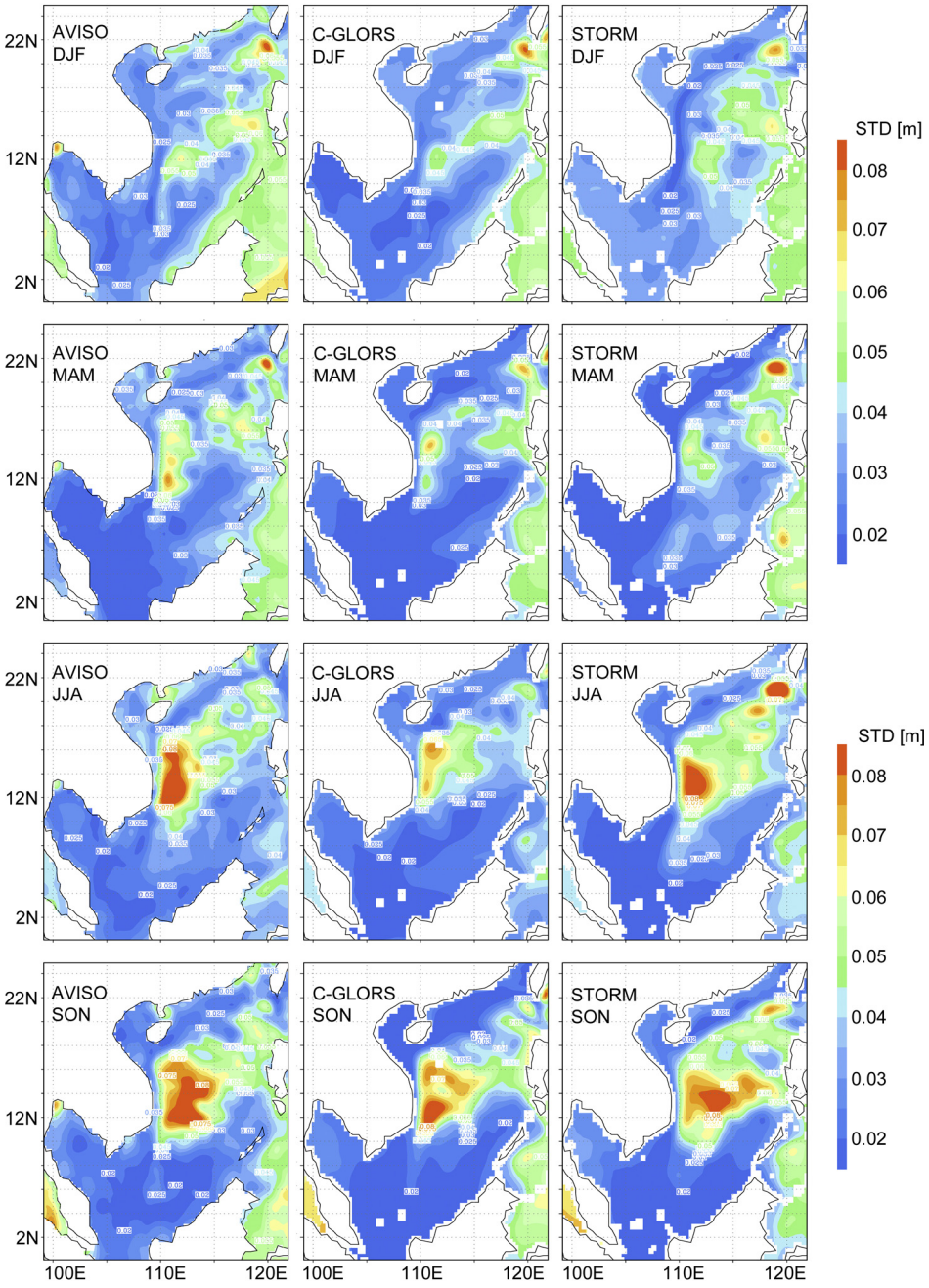

Figure 2 1993–2010 standard deviations (STD) [m] of seasonal detrended SSHA according to AVISO, C-GLORS and STORM. From top to bottom: DJF, MAM, JJA and SON.

In winter, strong counterclockwise currents dominate the southern SCS. The Kuroshio intrudes through the Luzon Strait from east to west and then divides into two branches, with the smaller one moving northward into the Taiwan Strait, the bigger one moving westward and then turning southward as a strong western boundary current along the coast. High-speed currents take place in the Luzon Strait, along the western boundary of the SCS (especially along the east coast of Malay Peninsula), and in the large cyclonic eddy of the southern SCS.

In summer, the strong currents along western boundary turn northward, which is consistent with the SCS monsoon, and clockwise currents occupy the southern SCS. At the same time, a strong flow offshore the Vietnam meanders to the central SCS and another flows northward along the southeast coast of China. In spring and autumn, two cyclonic eddies locate in the northern and southern SCS respectively. The seasonal patterns presented in STORM and C-GLORS are alike. But, the speeds in STORM are generally higher than those in C-GLORS, which may be due to the higher spatial resolution of STORM which may allow the simulation of more small-scale phenomena.

The EOFs of sea surface current (after subtracting the annual cycle) from the two data sets show similar inter-annual variability and explain the similar variance (11.9% in C_GLORS and 9.2% in STORM). The main features of the EOF1 patterns from both two data are the strong alongshore

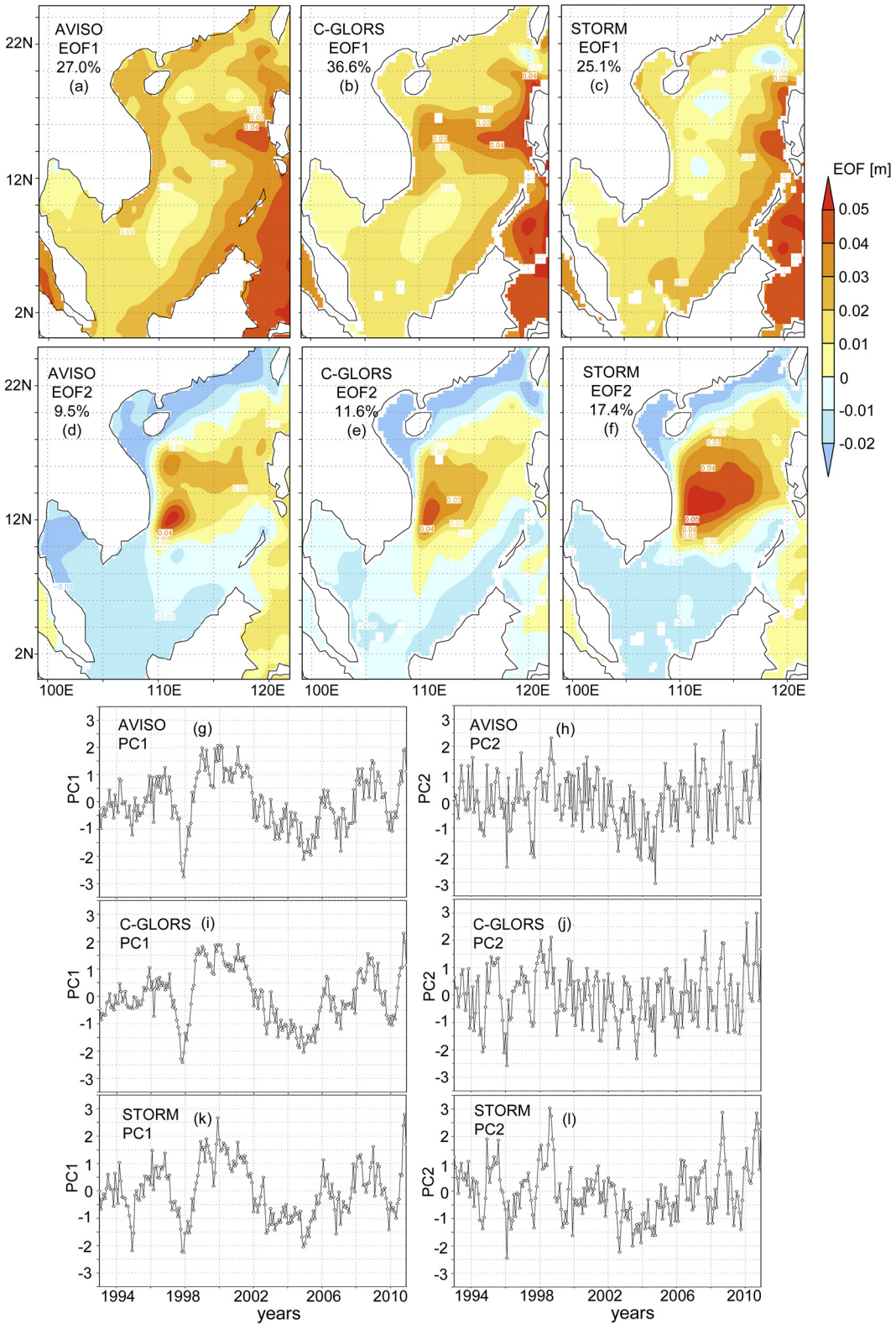

Figure 3 (a–f) The first two EOFs [m] of 1993–2010 monthly detrended SSHA (removing mean annual cycle) according to AVISO, C-GLORS and STORM. From top to bottom: EOF1 and EOF2. (g–l) The time coefficients for the first two EOFs of AVISO (top), C-GLORS (middle) and STORM (bottom), after detrending and subtraction of the mean annual cycle. From left to right: EOF1 and EOF2.

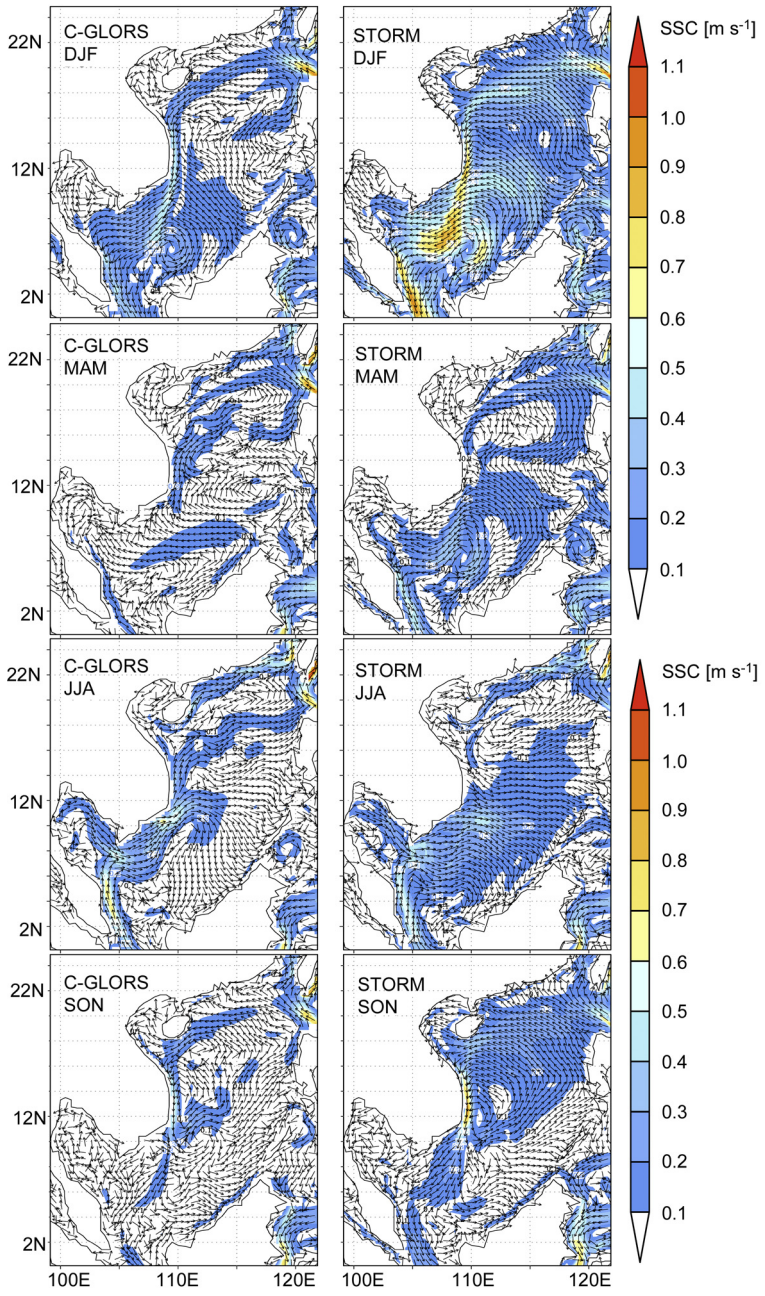

Figure 4 1982–2010 seasonal mean of sea surface currents (SSC; at 6 m depth) [m s^{-1}] according to C-GLORS and STORM. From top to bottom: DJF, MAM, JJA and SON.

southward currents and a gyre located in the middle SCS. The currents intrude into the SCS from the Pacific through the Luzon Strait and flow into the Pacific through the passage at the south of Philippines. The current speeds in STORM are a little higher than in C-GLORS for the region with slow (less than 0.02 m s^{-1}) currents.

3.3. SST in C-GLORS and STORM datasets

The distribution of SST can be deeply influenced by the ocean currents and its variance can be regarded as an important indicator of current variability, including vertical currents. In this section, SST is considered for evaluating the ability of the STORM dataset to reproduce the SCS dynamics.

The distributions of SST in the SCS (Fig. 5) show obvious seasonal differences. In winter, spring and autumn, most isotherms show northeast-southwest direction. The closer the area is to the Equator, the hotter the sea surface is. The SST in the SCS in summer is almost uniform but, with marked small upwelling regions in the southeast of China and near Vietnam. Previous studies (Fang et al., 2012; Wang et al., 2012, 2014; Xie et al., 2003) have demonstrated the presence of regional upwelling, which brings much colder water from deeper layer to the surface. STORM generates higher temperatures in summer in most regions, and it presents a stronger upwelling with larger temperature gradient than C-GLORS. The area with coldest seawater and largest gradient off the Southeast Vietnam coast is very close to the

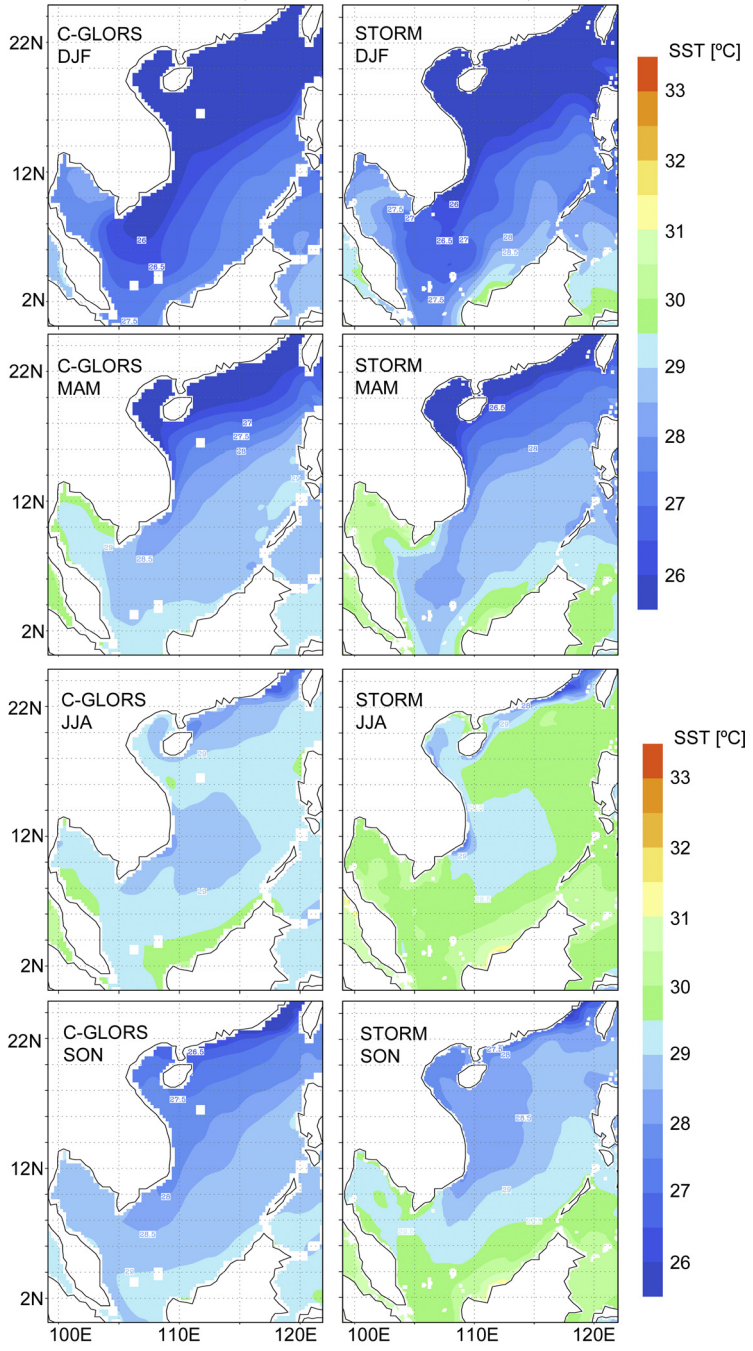

Figure 5 1982—2010 seasonal means of sea surface temperature (SST) [°C] according to C-GLORS and STORM. From top to bottom: DJF, MAM, JJA and SON.

land, then, with the limitation of horizontal resolution, C-GLORS may not be able to resolve these very small-scale phenomena. So STORM has an advantage in this case. The study of Tim et al. (2015) has found similarly colder SST in STORM compared with coarser observations in the South Atlantic.

4. A case of regional ocean downscaling

According to the assessment above, the capability of STORM to describe the large-scale state and small-scale variability has been verified. STORM is forced with atmospheric states given by NCEP, which is believed to be mostly homogenous since 1958 in describing "large-scale" (regional) variability. Thus, the STORM data set should be suitable for building empirical downscaling models for specifying regional and local phenomena and their statistics in the ocean.

For demonstrating this option, we have built one empirical downscaling model, as an example. As predictand we use the surface throughflow in the South China Sea and its neighboring seas (0—25°N, 99°—122°E), as given by the time series of the 1st EOF of deseasonalized monthly currents on the 0.25° grid (Fig. 6); as predictors the monthly wind speed

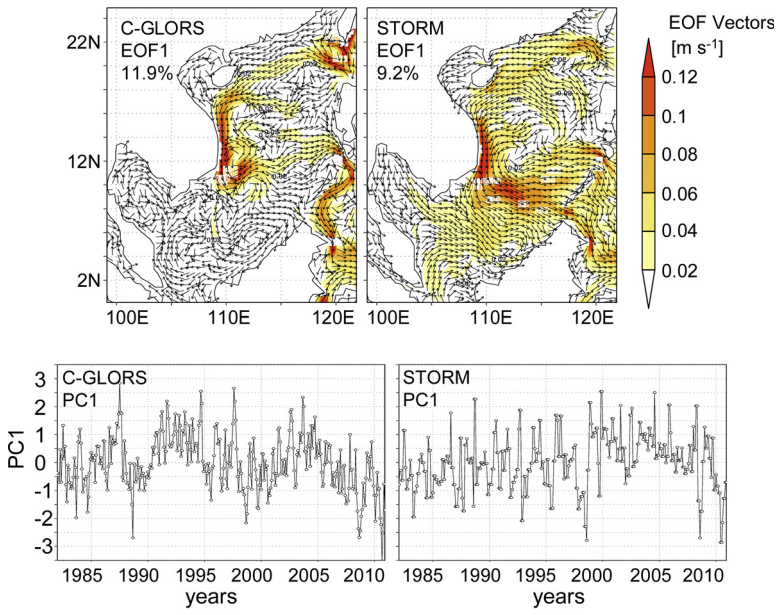

Figure 6 The first vector EOF [m s^{-1}] and the corresponding coefficient of 1982–2010 monthly sea surface currents (SSC; at 6 m depth) according to C-GLORS and STORM.

at 10 m height (0–25°N, 99°–122°E, including the land) as given by the 2.5° gridded NCEP re-analysis. The empirical model linking the predictors and the predictand is multiple linear regression (MLR).

As the instability of the quality of the NCEP1 before the year 1958, this experiment is performed during the period of 1958–2010. We choose the first 33 years (with 396 months) as the training period to construct the model and the last 20 years (with 240 months) as validation period.

There are several preparational steps to pre-process the data:

1. First, the annual cycle in both the predictors and the predictands are removed for both two periods.
2. Second, for the training period 1958–1990, after detrending the data, we get the first principal component PC1_C of the detrended and de-seasonalized currents C, and the principal components PCs_W of the detrended and de-seasonalized winds W. The pattern EOF1_C (not shown) presents almost the same pattern as that one given in Fig. 6. Using these PCs, we build the MLR models.
3. Third, for the validation period, the currents (and winds) are projected on EOF1_C (EOFs_W) to generate the pre-

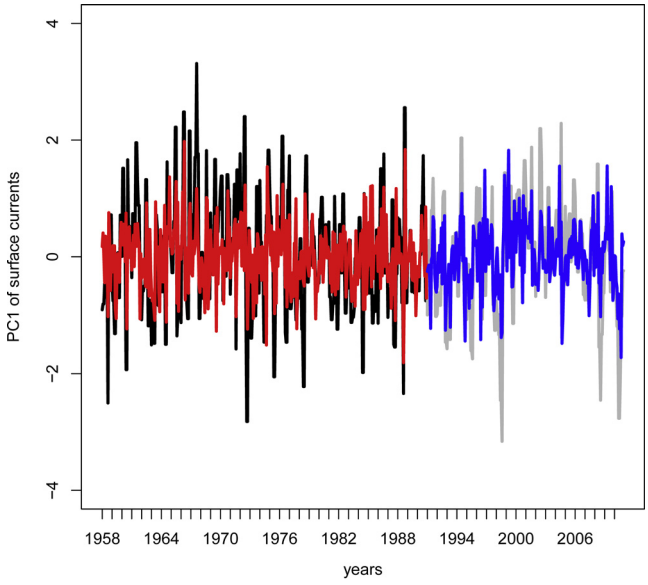

Figure 7 The original PC1 (the black line and the gray line) and the fitted PC1 (the red line and the blue line) of the surface currents for the training period and the validation period.

dictand PC1_C and the predictors PCs_W. The skill of the MLR model can be assessed by "predicting" PC1_C in the validation period by feeding the MLR model with the predictors PCs_W.

The number of PCs of predictors to be used for the construction of the downscaling model has an effect on the model skill. Too many PCs involved in the construction may result in the overfitted problem (Titus et al., 2013). After some tests, we find that the first 3 PCs of wind as predictors for the model construction performs well. The original PC1 and the fitted PC1 for both the training period and the validation period are shown in Fig. 7. The correlation coefficients between the predictand and the predicted PC1_C amounts to 0.55 in the training period 1958—1990, and 0.66 in the validation period (1991—2010).

The regressed predictand exhibits a similar, albeit smaller, variability to that one during the training period. We conclude that the multiple linear regression based on the principal component is good enough to build the statistical model to predict the non-seasonal variability of surface currents in the SCS.

5. Conclusions

Often, studies on the statistics of meso-scale SCS dynamics and scale-interactions suffer from insufficient observations in terms of spatial resolution and temporal coverage. One way of overcoming this limitation is to build empirical downscaling models for regional and local oceanic phenomena. A major problem for doing so is the availability of suitable data sets for constructing such empirical models.

One approach for solving this problem is to use multi-decadal simulations with high-resolution ocean models forced by atmospheric reanalyzes. For instance, the German consortium STORM project has produced a global high-resolution ocean dataset STORM, integrated with atmospheric forcing for the time period 1950—2010 and a one-tenth degree horizontal resolution. This dataset is found to generate realistically the variability on large and small scales in the SCS and statistics of small-scale features of the SCS dynamics. Using this data set, we built a statistical models of the links between large and small scales in the SCS, i.e. an empirical downscaling model.

For determining the STORM data as suitable, we introduce the global gridded AVISO satellite observations and the ocean re-analysis dataset C-GLORS in this study to evaluate the ability of STORM to reproduce the SCS dynamical structure. As C-GLORS have much more parameters than AVISO, for the joint period and the shared variable SSHA, we first verified the quality of C-GLORS and STORM. After that, we regard C-GLORS as "observations" to carry out the assessment of other variables (surface currents and SST) generated by STORM.

Overall, STORM and C-GLORS show good agreement with AVISO in reconstructing the SCS dynamical characteristics. The seasonal variability of SSHA resolved from STORM is very close to AVISO with the maximum center in the same locations, even though C-GLORS having assimilated the AVISO altimeter data is closer. The distributions of maximum SSHA standard deviation for four seasons from the three datasets are alike, but C-GLORS and STORM differ from the observed distribution, with respect to the intensity in winter and spring, the area of strong inter-annual variability in summer and autumn off the southeast Vietnam. The EOF decomposition of SSHA identifies similar patterns of interannual variability. A difference is that emergence of several small opposite centers far away from the coastline presented in EOF1 patterns of C-GLORS and STORM. The reason is not clear.

STORM hindcasts the same seasonal upper circulation and inter-annual variability as C-GLORS, however, it generates stronger current intensity, which may be caused by the increase in resolution. As for SST, even though STORM still overestimates the SST for most areas, the temperature distribution of STORM shows great similarity with C-GLORS, with colder temperature off the Vietnam coast (the strong upwelling area) in summer. The STORM description of the SCS circulation and some small-scale phenomena near coastline, for instance upwelling, is quite satisfactory.

A major albeit technical advantage of STORM is not only the availability of more dynamical variables, but also the longer time period, namely 1950, or 1958, until 2010.

Taking advantage of STORM, one statistical downscaling model has been built successfully to estimate the non-seasonal variability of the SCS surface currents for the past 60 years. The multiple linear regression based on the principal component shows skill.

While this downscaling model is merely an example demonstrating the potential, further downscaling models will be built in this spirit on the regional and local phenomena in the South China Sea, related to the formation of eddies, to coastal upwelling and other phenomena. These models may then also be used to derive scenarios of possible future change but also to change prior to 1950.

Acknowledgments

We thank the Helmholtz-Zentrum Geesthacht (HZG) for supporting the authors' research and the Chinese Scholarship Council (No. 201406330048) for funding the first author's studying abroad at the HZG. The authors are grateful to the Max Planck Institute of Meteorology (MPI) for providing the STORM simulations and to the Euro-Mediterranean Center for Climate Change (CMCC) for providing the C-GLORS data set, and we appreciate their suggestions.

References

AVISO, 1996. AVISO User Handbook Merged Topex/Poseidon Products (GDR-Ms), AVI-NT-02-101-CN Edn. 3.0, Romonville St-Agne, France, 199 pp.

AVISO, 2009. SSALTO/DUACS User Handbook: (M) SLA and (M) ADT Near-real Time and Delayed Time Products, Reference: CLS-DOS-NT-06-034, 29 pp.

Benestad, R.E., Hanssen-Bauer, I., Chen, D., 2008. Empirical-statistical Downscaling. World Scientific Publishing Company Incorporated, Singapore, 228 pp.

Cheng, X.H., Xie, S.P., Du, Y., Wang, J., Chen, X., Wang, J., 2016. Interannual-to-decadal variability and trends of sea level in the South China Sea. Clim. Dyn. 46 (9), 3113—3126, http://dx.doi.org/10.1007/s00382-015-2756-1.

Cui, M.C., von Storch, H., Zorita, E., 1995. Coastal sea-level and the large-scale climate state — a downscaling exercise for the

Japanese islands. Tellus Ser. A 47 (1), 132—144, http://dx.doi.org/10.1034/j.1600-0870.1995.00008.x.

Dale, W.L., 1956. Wind and drift currents in the South China Sea. Malays. J. Trop. Geogr. 8, 1—31.

Fang, G.H., Chen, H.Y., Wei, Z.X., Wang, Y.G., Wang, X.Y., Li, C.Y., 2006b. Trends and interannual variability of the South China Sea surface winds, surface height, and surface temperature in the recent decade. J. Geophys. Res. 111 (C11S16), 2156—2202, http://dx.doi.org/10.1029/2005JC003276.

Fang, W.D., Guo, J.J., Shi, P., Mao, Q.W., 2006a. Low frequency variability of South China Sea surface circulation from 11 years of satellite altimeter data. Geophys. Res. Lett. C11S16, http://dx.doi.org/10.1029/2006GL027431.

Fang, G.H., Wang, G., Fang, Y., Fang, W.D., 2012. A review on the South China Sea western boundary current. Acta Oceanolog. Sin. 31 (5), 1—10, http://dx.doi.org/10.1007/s13131-012-0231-y.

Ho, C.R., Zheng, Q.N., Soong, Y.S., Kuo, N.J., Hu, J.H., 2000. Seasonal variability of sea surface height in the South China Sea observed with TOPEX/Poseidon altimeter data. J. Geophys. Res. Oceans 105 (C6), 13981—13990, http://dx.doi.org/10.1029/2000JC900001.

Hu, J., Kawamura, H., Hong, H., Qi, Y., 2000. A review on the currents in the South China Sea: seasonal circulation, South China Sea warm current and Kuroshio intrusion. J. Oceanogr. 56 (6), 607—624, http://dx.doi.org/10.1023/A:1011117531252.

IPCC, 2013. Summary for Policymakers. In: Climate Change 2013: The Physical Science Basis. Contribution of Working Group I to the Fifth Assessment Report of the Intergovernmental Panel on Climate Change, Cambridge Univ. Press, Cambridge, United Kingdom/New York, USA, 10—11.

Kauker, F., von Storch, H., 2000. Statistics of "synoptic circulation weather" in the North Sea as derived from a multiannual OGCM simulation. J. Phys. Oceanogr. 30 (12), 3039—3049, http://dx.doi.org/10.1175/1520-0485(2000)030<3039:SOSCWI>2.0.CO;2.

Li, H.M., von Storch, J.S., 2013. On the fluctuating buoyancy fluxes simulated in a 1/10 degrees OGCM. J. Phys. Oceanogr. 43 (7), 1270—1287, http://dx.doi.org/10.1175/JPO-D-12-080.1.

Li, L., Xu, J.D., Jing, C.S., Wu, R.S., Guo, X.G., 2003. Annual variation of sea surface height, dynamic topography and circulation in the South China Sea — a TOPEX/Poseidon satellite altimetry study. Sci. China Ser. D 46 (2), 127—138.

Schrum, C., Siegismund, F., John, M., 2003. Decadal variations in the stratification and circulation patterns of the North Sea. Are the 1990 unusual? ICES Mar. Sci. Sympos. 121—131.

Storto, A., Masina, S., 2014. Validation of the CMCC Global Ocean Eddy-Permitting Reanalysis (C-GLORS). Centro Euro-Mediterraneo sui Cambiamenti Climatici, Bologna, Italy, 11 pp.

Storto, A., Masina, S., Navarra, A., 2016. Evaluation of the CMCC eddy-permitting global ocean physical reanalysis system (C-GLORS, 1982—2012) and its assimilation components. Q. J. R. Meteorolog. Soc. 142 (695), 738—758, http://dx.doi.org/10.1002/qj.2673.

Tim, N., Zorita, E., Hunicke, B., 2015. Decadal variability and trends of the Benguela upwelling system as simulated in a high-resolution ocean simulation. Ocean Sci. 11 (3), 483—502, http://dx.doi.org/10.5194/os-11-483-2015.

Titus, M.L., Sheng, J., Greatbatch, R.J., Folkins, I., 2013. Improving statistical downscaling of general circulation models. Atmos. Ocean 51 (2), 213—225, http://dx.doi.org/10.1080/07055900.2013.774259.

von Storch, H., Reichardt, H., 1997. A scenario of storm surge statistics for the German bight at the expected time of doubled atmospheric carbon dioxide concentration. J. Clim. 10 (10), 2653—2662, http://dx.doi.org/10.1175/1520-0442(1997)010<2653:ASOSSS>2.0.CO;2.

von Storch, H., Zwiers, F.W., 1999. Statistical Analysis in Climate Research. Cambridge Univ. Press, 293—305.

von Storch, H., Zorita, E., Cubasch, U., 1993. Downscaling of global climate-change estimates to regional scales — an application to Iberian rainfall in wintertime. J. Clim. 6 (6), 1161—1171, http://dx.doi.org/10.1175/1520-0442(1993)006<1161:DOGCCE>2.0.CO;2.

von Storch, J.-S., Eden, C., Fast, I., Haak, H., Hernández-Deckers, D., Maier-Reimer, E., Marotzke, J., Stammer, D., 2012. An estimate of the Lorenz energy cycle for the world ocean based on the STORM/NCEP simulation. J. Phys. Oceanogr. 42 (12), 2185—2205, http://dx.doi.org/10.1175/JPO-D-12-079.1.

Wang, Y., Fang, G., Wei, Z., Qiao, F., Chen, H., 2006. Interannual variation of the South China Sea circulation and its relation to El Niño, as seen from a variable grid global ocean model. J. Geophys. Res. 111, C11S14, http://dx.doi.org/10.1029/2005JC003269.

Wang, D.X., Zhuang, W., Xie, S.P., Hu, J.Y., Shu, Y.Q., Wu, R.S., 2012. Coastal upwelling in summer 2000 in the northeastern South China Sea. J. Geophys. Res. Oceans 117, C04009, http://dx.doi.org/10.1029/2011JC007465.

Wang, D.X., Shu, Y.Q., Xue, H.J., Hu, J.Y., Chen, J., Zhuang, W., Zu, T.T., Xu, J.D., 2014. Relative contributions of local wind and topography to the coastal upwelling intensity in the northern South China Sea. J. Geophys. Res. Oceans 119 (4), 2550—2567, http://dx.doi.org/10.1002/2013JC009172.

Wei, Z.X., Fang, G.H., Choi, B.H., Fang, Y., He, Y.J., 2003. Sea surface height and transport stream function of the South China Sea from a variable-grid global ocean circulation model. Sci. China Ser. D 46 (2), 139—148, http://dx.doi.org/10.3969/j.issn.1674-7313.2003.02.005.

Wyrtki, K., 1961. Physical Oceanography of the Southeast Asian Waters, Scientific Results of Marine Investigations of the South China Sea and the Gulf of Thailand, NAGA Rep. 2. Scripps Inst. Oceanogr., La Jolla, CA, 195 pp.

Xie, S.P., Xie, Q., Wang, D.X., Liu, W.T., 2003. Summer upwelling in the South China Sea and its role in regional climate variations. J. Geophys. Res. Oceans 108, C83261, http://dx.doi.org/10.1029/2003JC001867.